Supporting Information

QM/MM study of the taxadiene synthase mechanism

*Jeaphianne P. M. van Rijn, Andrés M. Escorcia and Walter Thiel**

*W.T.: Max-Planck-Institut für Kohlenforschung, Kaiser-Wilhelm-Platz 1, 45470 Mülheim, Germany. Email: thiel@kofo.mpg.de

Content:

1. Method and system setup

Table S1 Reaction coordinates used in the QM/MM PES scans to obtain the reaction profiles of the conversion of ^{TXS}GGPP to ^{TXS}**T** and side products[1]

Reaction step	**Reaction coordinate used for scan**
GGPP-A	O1-C1 distance
A-C	C1-C14 distance
C-F_{chair}	(C10-H10) – (H10-C2) distance difference
C-$D1_{chair}$	(C10-H10) – (H10-C6) distance difference
F_{chair}-F_{boat}	Dihedral angle C12-C13-C14-C15
F_{chair}-$D1_{chair}$ / F_{boat}-$D1_{boat}$	(C2-H10) – (H10-C6) distance difference
$D1_{boat}$-$D2_{boat}$	Dihedral angles C3-C4-C5-C6 and C4-C5-C6-C7 (simultaneously)
$D2_{boat}$-E_{C_chair}	C2-C7 distance
E_{C_chair}-E_{C_boat}	Dihedral angle C20-C3-C4-C5
E_{C_boat}-$E2_{C\_boat}$	O1-C4:Hβ distance
$E2_{C\_boat}$ -T	O1- C4:Hβ distance
$E2_{C\_boat}$ -T1	(C20:H^2-C20) - (O1-C20:H^2) distance difference
C-H_2O-V	(C12:H^2-C12) - (O_w-C12:H^2) distance difference [3]
F_{chair}/F_{boat}-V1	(C20:H^2-C20) - (O1-C20:H^2) distance difference
F_{boat} -V2	(C2:H^2-C2) - (O1-C2:H^2) distance difference
F_{chair}/F_{boat}-H_2O-V2	(C2:H^2-C2) - (O_w -C2:H^2) distance difference [3]

[1] Atom labels can be found in Figures 1 and 3 of the main text
[2] Hydrogen atom closest to base (PPi:O1).
[3] Water-mediated proton transfer reaction from cation to PPi. The concomitant decrease of the H_w-PPi:O1 distance occurred spontaneously when varying the indicated reaction coordinate.

IRC-like calculation

An IRC-like calculation makes use of an approximate IRC procedure. In an IRC-like calculation, a fraction of the normal mode eigenvector corresponding to the imaginary frequency of the transition state is added to (or subtracted from) the structure of the transition state. The new structure is subjected to an unconstrained geometry optimization, and the resulting structure is visually inspected to confirm that it is the reactant or product.

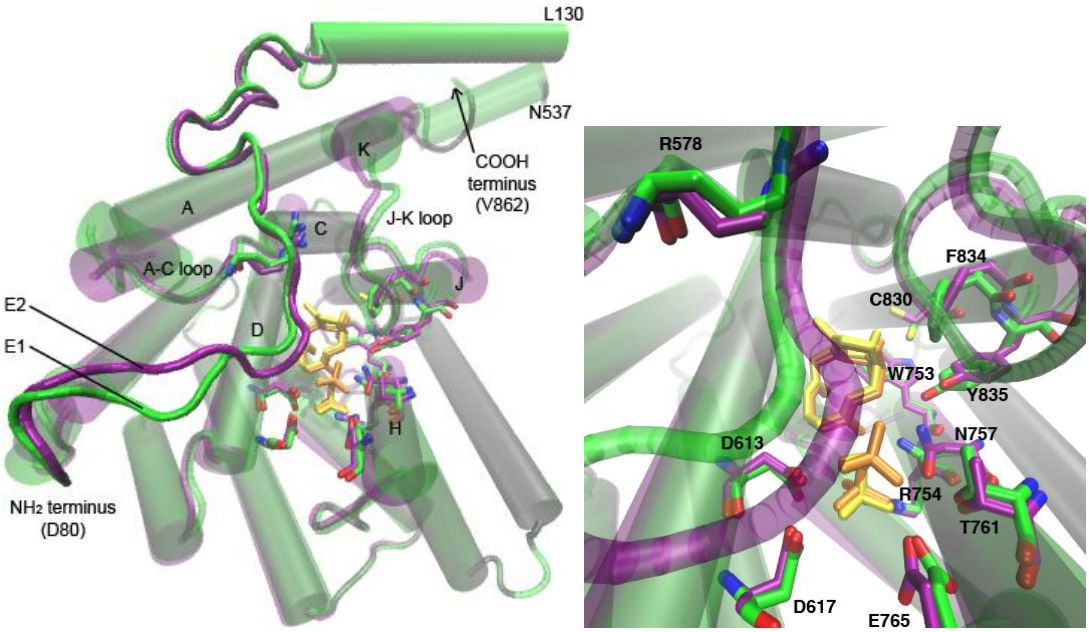

Figure S1. Left: Structure of the entire enzyme for snapshot W1E1:**C** (green) and W2E2:**C** (purple) comprising the C-terminal domain (S553-V862) and part of the N-terminal domain (D80-L130 and N537-Q552). Right: Zoom of the active site with a selection of the residues responsible for positioning of the PPi anion (D613, D617, R754, N757, T761, E765) or positioning of cation **C** (W753, C830, F834, Y835).

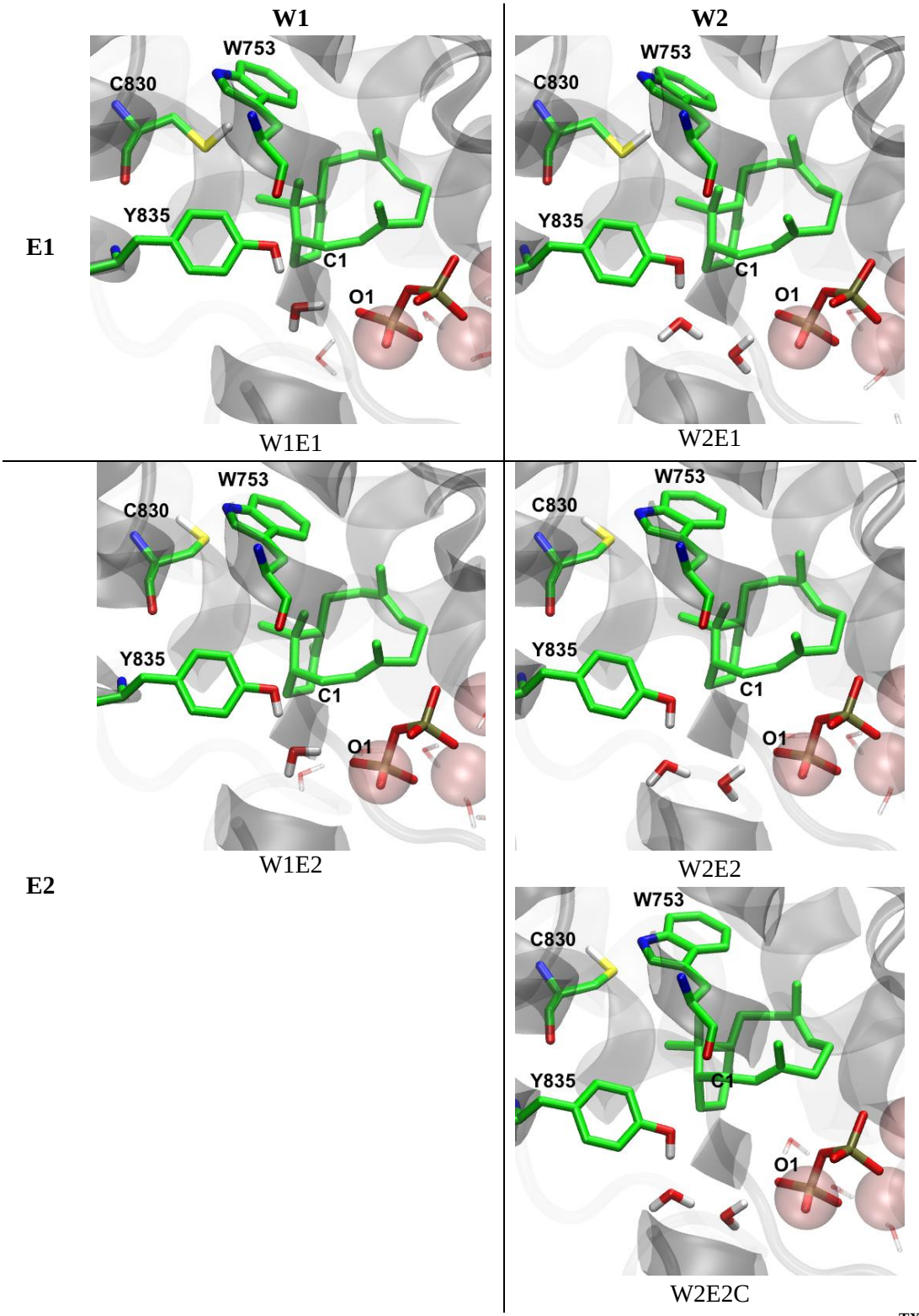

Figure S2 The five different setups **C:**WxEx taken from the MD simulation of the ^{TXS}**C** complex [1]. There are one (W1) or two (W2) water molecules between Y835 and PPi:O1. C830 interacts with W753 (E1) or C830 points away from W753 (E2). Most hydrogen atoms are omitted for clarity.

2. Results of QM study

Table S2

QM energies relative to cation **C** (ΔE in kcal/mol) for single-point calculations and for (re)optimizations of the published HT-QM structures[2] with different methods.[1]

Stationary Point	Method							
	Re-optimized structures					Single-point calculations		
	B3LYP/6-31+G(d,p)	B3LYP-D/6-31+G(d,p)	ωB97xD/6-31+G(d,p)	M06-2X/6-31+G(d,p)	M06-2X/TZVP	M06-2X/6-31+G(d,p)	mPW1PW91/ 6-31+G(d,p)[2]	DLPNO-CCSD(T)/ def2-TZVPP[2]
A	15.5	25.6	35.3	32.5	31.4	35.9	29.3	37.3
TS(A-B)	17.7	DNC	DNC	DNC	DNC	DNC	29.3	DNC
B	12.5	17.1	22.7	21.4	21.0	22.9	19.1	25.3
TS(B-C)	14.8	19.4	DNC	21.6	21.2	DNC	23.2	24.5
C	0.0	0.0	0.0	0.0	0.0	0.0	0.0	0.0
TS(C-D1)	13.2	10.2	13.3	11.4	11.5	11.3	11.0	14.0
TS(C-F)	8.6	6.5	9.3	7.4	7.8	8.0	6.5	10.2
F	0.6	0.3	1.0	0.4	0.6	1.6	0.4	2.2
TS(F-D1)	8.0	6.6	8.8	7.2	7.7	7.2	6.0	9.8
D1	2.4	1.9	2.3	1.9	2.1	2.8	2.1	3.0
TS(D1-D2)	6.0	6.5	5.9	4.9	4.9	5.1	6.5	6.6
D2	5.3	5.3	7.5	5.7	6.0	5.8	5.4	6.5
TS(D2-E)	11.9	DNC	10.3	5.9	8.6	8.2	8.2	DNC
E	11.2	10.0	6.1	5.2	6.0	5.3	5.7	1.9

[1] DNC = calculation does not converge

[2] Reported relative energies do not include ZPE corrections.

The published HT-QM structures[2] were re-optimized with different methods (see Method section in the main text and Table S1). For cation **A** the structures obtained with M06-2X/6-31+G(d,p) and M06-2X/TZVP deviated from the HT-QM structure with an RMSD of 0.37 Å for the aligned carbon atoms. For cation **B** the structure is already more similar to the HT-QM structure (RMSD of 0.12 Å) and the further the reaction progresses, the smaller the differences between the HT-QM (starting) structure and the re-optimized structure, indicated by RMSD values of 0.06 Å and less for cation **D2** and cation **E**.

Because of conformational changes during re-optimization, a connected pathway between the optimized structures of cation **A** and cation **E** is no longer guaranteed, and optimizations for the transition states TS(A-B), TS(B-C), and TS(D1-D2) do not converge at all levels of theory applied. For comparison to QM/MM data we therefore use the data from the M06-2X/6-31+G(d,p) single-point calculations. Comparison of the results for M06-2X/6-31+G(d,p) and M06-2X/TZVP shows that basis set effects are generally small.

Table S3

QM energies relative to cation $\mathbf{C_{chair}}$ (ΔE in kcal/mol) for structures of different cations optimized with the A ring (**C**, **F**, **D1**, and **D2**) and the C ring (**E** and **E2**) in chair-like and boat-like conformation.

Cation	Conformation of A or C ring			
	Chair		Boat	
	M06-2X/ 6-31+G(d,p) [1]	DLPNO-CCSD(T)/ def2-TZVPP[2]	M06-2X/ 6-31+G(d,p) [1]	DLPNO-CCSD(T)/ def2-TZVPP[2]
C	0.0	0.0	-0.1[3]	NC[5]
F	0.4	2.2	0.4[3]	NC[5]
D1	1.9	3.1	7.0	6.4
D2	5.7	6.5	5.9[3]	NC[5]
E	5.2	1.9	1.5	-2.8
E2	NC[6]	NC[6]	1.4[4]	-3.0[4]

[1] Optimizations start from the geometries of the cations as found in the QM/MM calculations.
[2] Single-point calculation on M06-2X/6-31+G(d,p) optimized structures. Relative energies do not include ZPE corrections.
[3] During optimization, the structure converts back to the chair-like conformation.
[4] Species $\mathbf{E_{C\_boat}}$ and $\mathbf{E2_{C\_boat}}$ differ in the orientation of the cation in the binding pocket. As expected, in the gas phase, their energies are comparable.
[5] NC = not calculated; these structures convert to chair-like conformation during optimization at the M06-2X level, and hence the expensive CCSD(T) calculations were not performed.
[6] $\mathbf{E2_{C\_chair}}$ is not observed in the QM/MM calculations.

Table S4

QM energies (ΔE in kcal/mol) for the different (side) products optimized with the A ring (products V-V2) and C ring (products T, T1) in chair-like and boat-like conformation.[1]

Product	Conformation of A or C ring			
	Chair		Boat	
	M06-2X/ 6-31+G(d,p) [2]	DLPNO-CCSD(T)/ def2-TZVPP[3]	M06-2X/ 6-31+G(d,p) [2]	DLPNO-CCSD(T)/ def2-TZVPP[1]
T	54.7	54.1	0.0	0.0
T1	6.0	5.1	3.3	3.4
V	-0.4	2.2	NC[4]	NC[4]
V1	3.6	5.7	8.4	10.5
V2	0.5	2.6	4.8	7.2

[1] Energies are given relative to the main product $\mathbf{T_{C\_boat}}$ (taxadiene with the C ring in boat-like conformation).
[2] Optimizations start from the geometries of the products as found in the QM/MM calculations.
[3] Singe-point calculations on M06-2X/6-31+G(d,p) optimized structures. Relative energies do not include ZPE corrections
[4] NC = not calculated. We did not find cation $^{\mathbf{TXS}}\mathbf{C_{boat}}$ which suggests that product $\mathbf{V_{boat}}$ may be unlikely.

3. GGPP → E QM/MM reaction profile

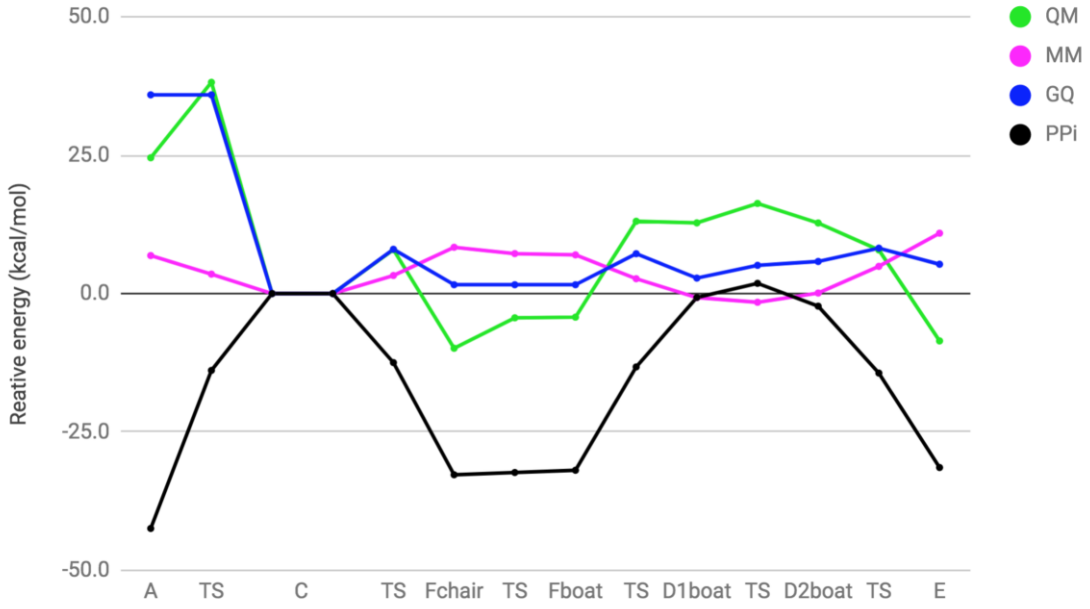

Figure S3

Partitioning of the QM/MM energy into QM (green) and MM (purple) components for setup W1E2 (see Figure S2). The QM energy component of the QM/MM energy includes the electrostatic interaction between the QM region and the MM region (electrostatic embedding, see Methods section in the main text). In black: contribution of PPi to the QM energy as calculated using an electrostatic perturbation approach[3]–[5]. In blue: the reference energies from M06-2X/6-31+G(d,p) single-point calculations on the HT-QM structures. Energies are given relative to cation **C**. A similar profile of the PPi energy contribution to the QM/MM reaction profile is expected for all other setups, since the variation of the interatomic distance between the center of the positive charge of the cations and PPi is similar along all computed reaction profiles.

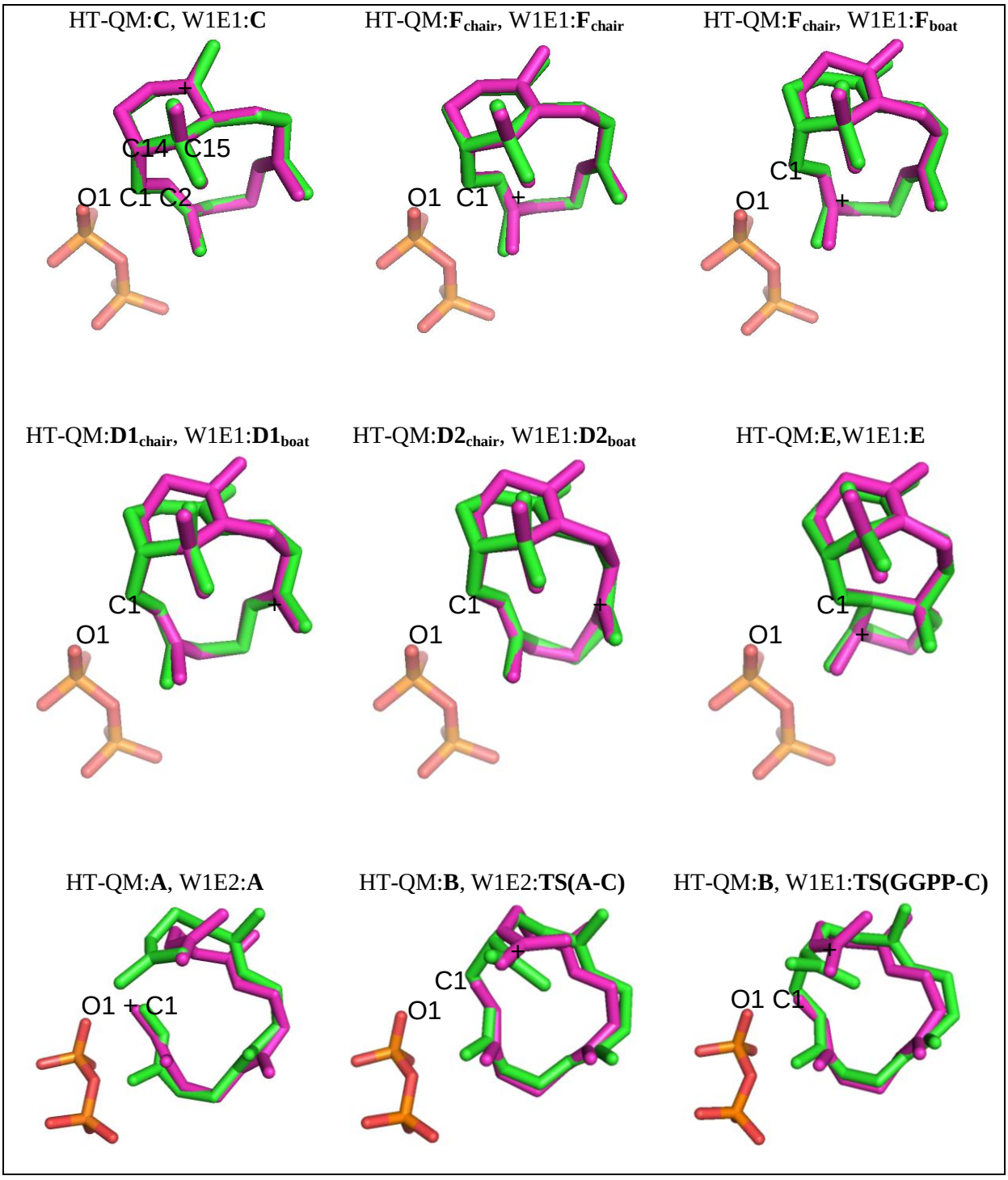

Figure S4
Overlay of HT-QM cation structures (green) and WxEx (see Figure S2) carbocation structures (magenta). Hydrogen atoms are omitted for clarity.

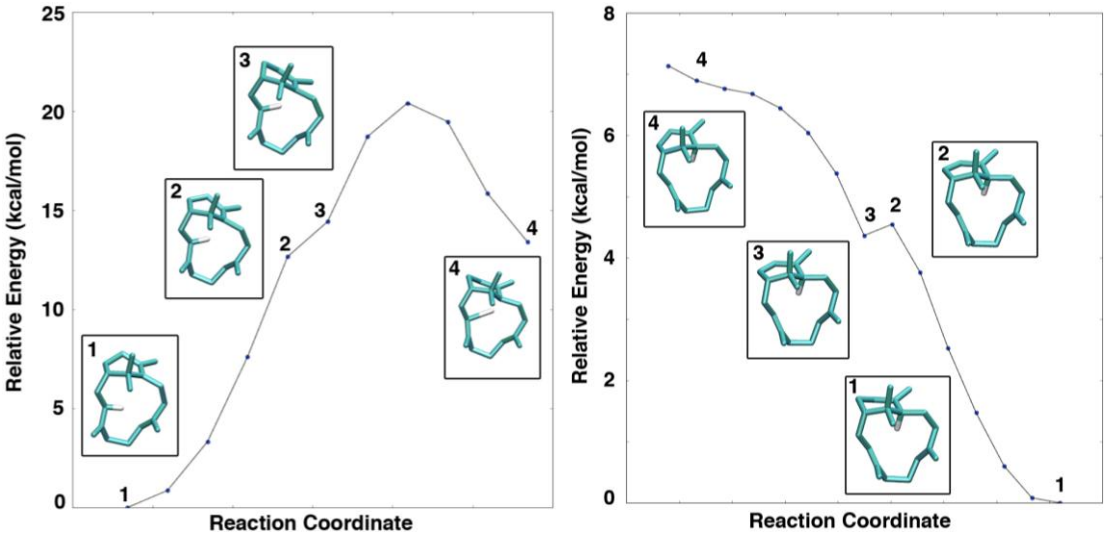

Figure S5

Left: scan from $\mathbf{F}_{\mathbf{boat}}$ to $\mathbf{C}_{\mathbf{boat}}$ for setup W1E1. Between points 2 and 3 the A ring changes from boat-like to chair-like conformation. Right: scan from $\mathbf{C}_{\mathbf{chair}}$ to $\mathbf{C}_{\mathbf{boat}}$ for setup W1E1. Though point 4 clearly is $\mathbf{C}_{\mathbf{boat}}$, it is not a minimum and optimization leads back to $\mathbf{C}_{\mathbf{chair}}$.

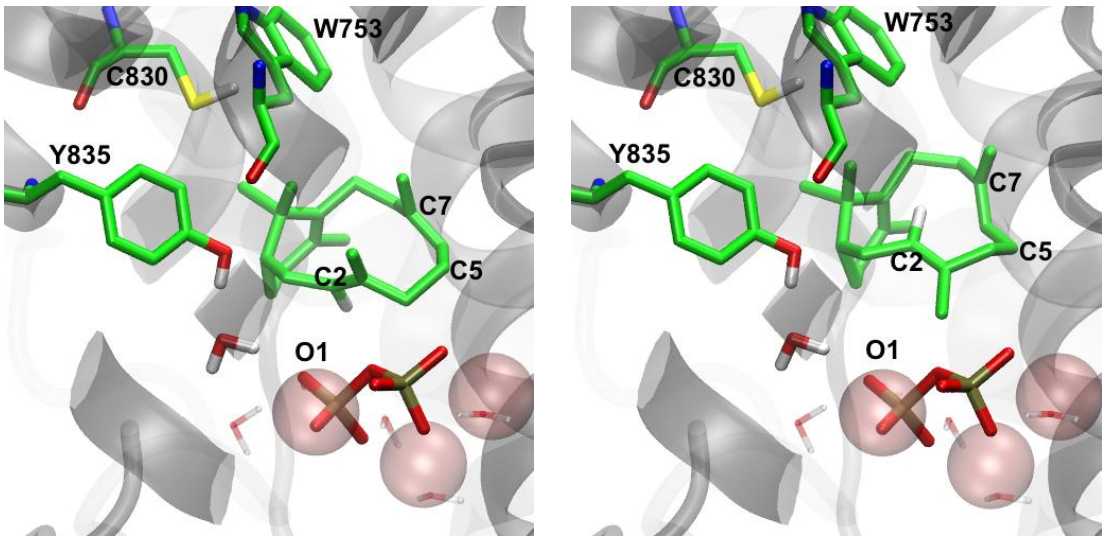

Figure S6

Left: W1E1:$\mathbf{D2}_{\mathbf{boat}}$ as observed on the catalytic pathway (see Figure 4 of the main text). Right: W1E1:$\mathbf{D2}_{\mathbf{boat}}$ after internal rotation around the C3-C4 bond. As can be seen, this will lead to the wrong orientation of H2 in the final product (see Figure 1 of the main text). Most hydrogen atoms are omitted for clarity.

Table S5

Important bond distances for positioning of the isopropyl tail of GGPP in the TXS binding pocket[1]

Distance	WxE1[2]	WxE2[3]	W1Ex[4]	W2Ex[5]
GGPP:C1 - GGPP:C14	3.6 (0.3)	3.9 (0.2)		
GGPP:C1 - GGPP:C15	4.6 (0.1)	5.0 (0.3)		
GGPP:C10 - GGPP:C15	3.1 (0.0)	3.3 (0.1)		
C830:S_C - GGPP:C15	4.1 (0.0)	5.1 (0.3)		
W753:C_W - GGPP:C15	5.3 (0.0)	5.0 (0.2)		
Y835:H_Y - GGPP:C15			3.8 (0.0)	3.3 (0.2)
F834:C_F- GGPP:C15			3.9 (0.0)	4.4 (0.2)

[1] Distances are giving in Å and correspond to average values as indicated below (standard deviations in parentheses). Labels can be found in Figure S7.

[2] Average over W1E1 and W2E1; [3] Average over W1E2, W2E2, and W2E2C; [4] Average over W1E1 and W1E2; [5] Average over W2E1, W2E2, and W2E2C.

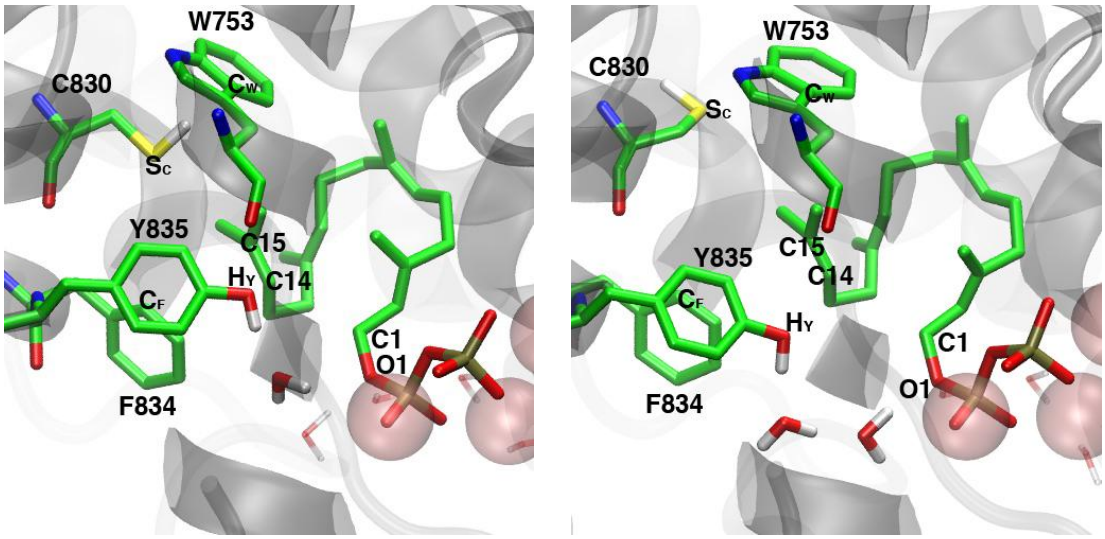

Figure S7

Left: W1E1:GGPP. Right: W2E2:GGPP. Most hydrogen atoms are omitted for clarity. When the thiol group of C830 interacts with W753 (left), the C1-C14 and C1-C15 distances are shorter than when the thiol is flipped (right). See Table S5 above.

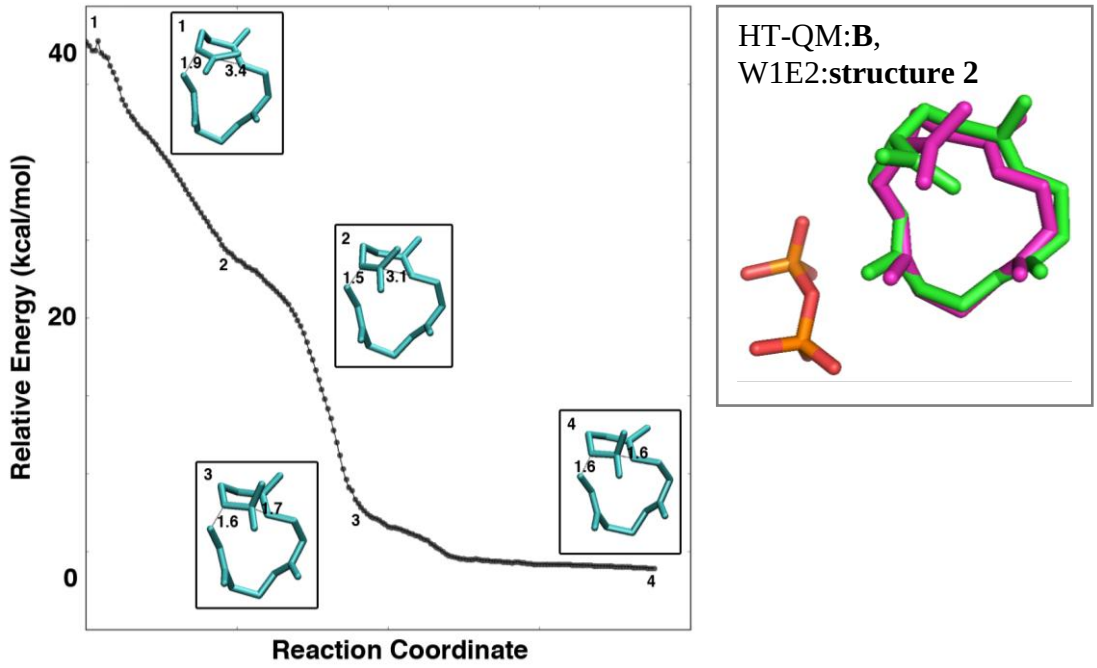

Figure S8

Optimization of W1E2:**TS(A-C)** passes through a structure similar to HT-QM cation **B**. Left: energy profile of IRC-like calculation from W1E2:**TS(A-C)** to W1E2:**C**. Right: Overlay of HT-QM cation **B** (green) and structure 2 from left scan (magenta). Hydrogen atoms are omitted for clarity.

Table S6

Average QM/MM energies (in kcal/mol with respect to the ^{TXS}**C** complex) of the computed energy profiles for the conversion of GGPP to **T** in the TXS environment. Also shown is the partitioning of the QM/MM energy into QM and MM components. Standard deviations are given in parentheses.

System[1]	Stationary point	QM	MM	QM/MM
WxE1[2]	GGPP	11.3 (9.8)	2.5 (6.4)	13.8 (3.5)
	TS(GGPP-C)	36.5 (3.8)	3.6 (0.1)	40.1 (3.9)
WxE2[3]	GGPP	15.1 (3.8)	1.6 (2.7)	16.8 (3.8)
	TS(GGPP-A)	33.8 (6.0)	-0.5 (6.6)	33.3 (1.7)
	A	24.0 (0.6)	6.6 (0.4)	30.7 (0.6)
	TS(A-C)	39.0 (1.3)	2.8 (1.0)	41.8 (1.9)
WxEx[4]	C	0.0 (0.0)	0.0 (0.0)	0.0 (0.0)
	TS(C-F_{chair})	7.5 (2.2)	3.7 (0.8)	11.2 (2.5)
	TS(C-$D1_{chair}$)	17.9 (4.0)	2.1 (4.1)	19.9 (1.3)
	$D1_{chair}$	5.0 (3.6)	2.7 (4.1)	7.6 (1.9)
	F_{chair}	-14.0 (3.0)	9.0 (1.7)	-5.0 (3.4)
	TS(F_{chair}-F_{boat})	-10.4 (4.2)	9.7 (2.3)	-0.7 (3.1)
	TS(F_{chair}-$D1_{chair}$)	4.3 (2.6)	5.4 (2.4)	9.6 (2.9)
	F_{boat}	-10.6 (4.0)	9.0 (2.0)	-1.6 (3.3)
	TS(F_{boat}-$D1_{boat}$)	7.3 (3.7)	4.8 (1.3)	12.1 (2.9)
	$D1_{boat}$	7.2 (3.8)	3.1 (2.3)	10.3 (2.4)
	TS($D1_{boat}$-$D2_{boat}$)	8.5 (5.0)	4.8 (4.2)	13.3 (1.9)
	$D2_{boat}$	4.9 (6.2)	5.9 (3.8)	10.8 (2.9)
	TS($D2_{boat}$-E_{C_chair})	2.0 (6.5)	8.6 (4.2)	10.6 (3.9)
	E_{C_chair}	-15.3 (7.3)	13.5 (6.2)	-1.7 (2.8)

[1] The pathway from ^{TXS}GGPP to ^{TXS}C contains one or two steps depending on the NTRC configuration and is therefore split for WxE1 and WxE2. See main text, section 3.1, Other setups.

[2] Averaged over W1E1 and W2E1.

[3] Averaged over W1E2, W2E2, and W2E2C.

[4] Averaged over W1E1,W2E1, W1E2, W2E2, and W2E2C.

Table S7

Average barriers and reaction energies (in kcal/mol) for the conformational and translational changes of cation **E** along the computed reaction profiles of the conversion of GGPP to **T** in the TXS environment. Standard deviations are given in parentheses.

Reaction step	System	Reaction energy	Reaction barrier
$E_{C\_chair} \rightarrow E_{C\_boat}$	WxE1[1]	1.2 (0.2)	19.2 (1.5)
	WxE2[2]	0.3 (0.4)	9.3 (1.7)
$E_{C\_boat} \rightarrow E2_{C\_boat}$	WxEx[3]	6.0 (7.3)	8.7 (5.6)

[1] Averaged over W1E1 and W2E1.

[2] Averaged over W1E2, W2E2 and W2E2C.

[3] Averaged over W1E1, W1E2 and W2E1. For W2E2 and W2E2C the $\mathbf{E_{C\_boat} \rightarrow E2_{C\_boat}}$ conversion was not found

Table S8

Important distances (in Å) for positioning (top) and deprotonation pathways (bottom) of the different conformations of cation **E** in the TXS binding pocket.[1]

Conformation and setup		Distance (Å)				
		$C830{:}S_C$ - $W753{:}C_W$	$C830{:}S_C$ - C15	$W753{:}C_W$- C15	$W753{:}C_W$- C16	PPi:O1- C20
E_{C_chair}	WxE1[2]	3.8 (0.2)	4.5 (0.1)	5.6 (0.1)	4.2 (0.1)	3.3 (0.2)
	W2E2x[3]	5.1 (0.1)	5.1 (0.2)	4.9 (0.0)	3.4 (0.0)	4.6 (0.0)
	W1E2	5.0	4.8	5.7	4.2	4.1
E_{C_boat}	WxE1[2]	3.8 (0.2)	4.5 (0.0)	5.6 (0.1)	4.1 (0.0)	3.1 (0.1)
	W2E2x[3]	5.2 (0.0)	4.8 (0.1)	4.6 (0.0)	3.6 (0.1)	4.2 (0.3)
	W1E2	5.1	4.8	5.7	4.2	3.0
$E2_{C\_boat}$	WxE1[2]	3.7 (0.2)	4.3 (0.2)	5.2 (0.5)	4.2 (0.5)	3.6 (0.6)
	W1E2	5.1	4.8	5.3	4.2	4.1

Conformation and setup		Distance (Å)				
		PPi:O1- H20[4]	PPi:O1- H4α	PPi:O1- H4β	PPi:O4- H4α	PPi:O4- H4β
E_{C_chair}	WxE1[2]	2.3 (0.3)	4.1 (0.5)	3.8 (0.0)	5.2 (0.6)	3.4 (0.5)
	W2E2x[3]	3.7 (0.1)	4.1 (0.2)	4.3 (0.1)	4.3 (0.1)	2.5 (0.1)
	W1E2	3.0	5.2	4.5	5.3	3.5
E_{C_boat}	WxE1[2]	2.3 (0.4)	4.4 (0.3)	5.0 (0.1)	3.0 (0.2)	4.4 (0.4)
	W2E2x[3]	3.1 (0.3)	4.7 (0.5)	5.9 (0.6)	2.6 (0.4)	2.8 (0.2)
	W1E2	2.6	4.9	4.4	4.4	2.9
$E2_{C\_boat}$	WxE1[2]	2.8 (0.8)	3.1 (0.1)	2.2 (0.1)	4.3 (0.0)	4.2 (0.2)
	W1E2	3.4	2.6	2.9	4.2	4.3

[1] Distances correspond to average values as indicated below. Standard deviations are given in parentheses. See Figs. S9-S10 for atom labels. [2] Average over W1E1 and W2E1. [3] Average over W2E2 and W2E2C. [4] Hydrogen atom closest to base (PPi:O1).

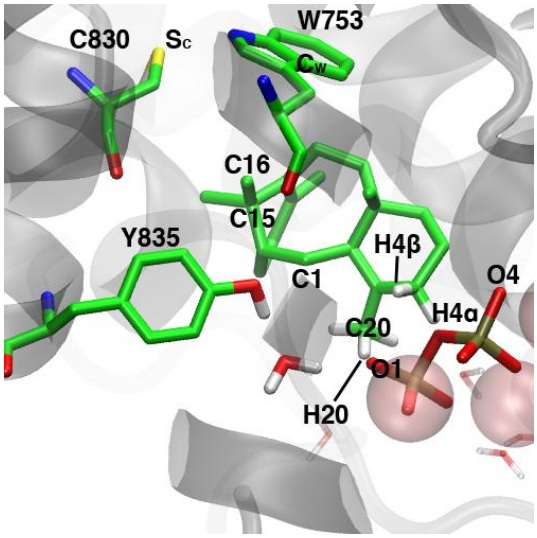

Figure S9

The $^{TXS}E2_{C\_boat}$ complex from snapshot W1E2E showing all relevant labels for Table S8.

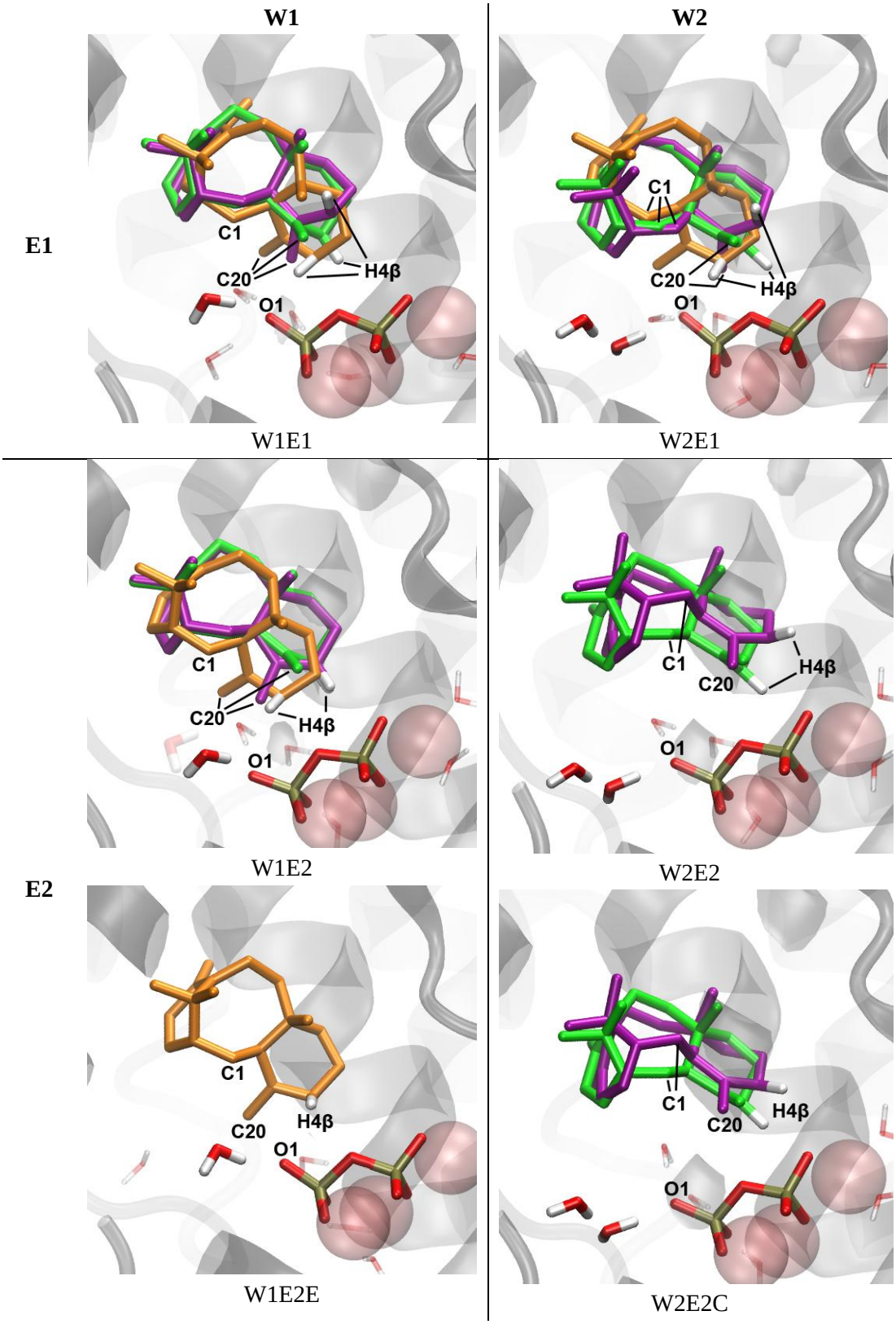

Figure S10
^{TXS}**E** complexes identified in the QM/MM calculations. ^{TXS}**E**$_{C\_chair}$ (cation in green) originates from the ^{TXS}**D2**$_{boat}$ complex. ^{TXS}**E**$_{C\_boat}$ (cation in purple) results from a conformational change of the C ring to boat-like conformation. ^{TXS}**E2**$_{C\_boat}$ (cation in orange) originates from a slight rotation of the **E**$_{C\_boat}$ conformer. All hydrogen atoms except for H4β are omitted for clarity. From the MD simulations of ^{TXS}**E**[1], an additional snapshot of ^{TXS}**E2**$_{C\_boat}$ was taken, W1E2E. The other snapshots correspond to setups described in Fig. S2.

Table S9
QM/MM energies (in kcal/mol) of the reaction profile computed for the conversion of **C** to **T** using the ^{TXS}**E2**$_{C\_boat}$ snapshot, W1E2E. For comparison, the data reported by Ansbacher et al.[6] using the FHM is shown. Energies are given relative to the ^{TXS}**C** complex[1].

	^{TXS}**E2**$_{C\_boat}$ snapshot, W1E2E			Ansbacher et. al.[6]
	QM	**MM**	**QM/MM**	
C	0.0	0.0	0.0	0.0
TS(C-F$_{boat}$)	8.6	2.0	10.6	4.9
TS(C-D1$_{boat}$)	6.4	2.8	9.2	4.0
F$_{boat}$	-15.2	5.7	-9.6	-9.9
TS(F$_{boat}$ -D1$_{boat}$)	4.9	3.6	8.5	6.6
D1$_{boat}$	-8.4	3.9	-4.6	-15.8
D2$_{boat}$	3.8	-2.9	0.9	Not reported[2]
TS(D2$_{boat}$ -E2$_{C_boat}$)	6.0	0.0	6.0	-11.0
E2$_{C_boat}$	-22.1	-6.7	-28.8	-24.4
TS(E2$_{C_boat}$ -T)	-21.0	-5.1	-26.1	-22.1
T	-51.5	6.0	-45.6	-34.8
TS(E2$_{C_boat}$ -T1)	-14.6	-8.0	-22.6	Not reported[2]
T1	-38.9	0.5	-38.4	Not reported[2]

[1] The ^{TXS}**C** complex found by back propagation for W1E2E has a different orientation in the binding pocket than the setups taken from the MD simulation of the ^{TXS}**C** complex[1] (see Table S10).
[2] An energy value for this complex is not reported in [6].

Table S10.
Distance (Å) between the center of positive charge of cations **C**, **D1** and **F** (CX^+)[1] and surrounding atoms (important for charge stabilization) in the QM/MM reaction profiles obtained for setups W1E1 and W1E2E.

Interatomic distance[1]	System					
	W1E1			W1E2E		
	C	D1$_{boat}$	F$_{boat}$	C	D1$_{boat}$	F$_{boat}$
CX^+-PPi:O1	6.2	7.4	3.5	7.8	5.1	4.1
CX^+-PPi:O2	7.5	7.4	3.6	8.6	5.2	5.6
CX^+-PPi:O4	9.2	8.0	5.0	9.8	6.1	7.6
CX^+-D613$_{OD1}$	9.3	7.6	4.8	9.3	5.9	7.1
CX^+-D613$_{OD2}$	8.3	7.7	5.3	8.8	6.0	5.9
CX^+-W753[2]	7.4	6.2	8.0	6.2	5.8	8.9
CX^+-Y841[2]	5.8	9.7	9.4	7.7	9.7	7.1

[1] X=11 for cation **C**; X=7 for cation **D1** and X=3 for cation **F**. Labels can be found in Fig. 3 of the main text and Figs. S12b and S12d.
[2] For W753 and Y841 we report the distance between CX^+ and the centroid of the heavy ring atoms.

4. Deprotonation data

Table S11
Average barriers and reaction energies (in kcal/mol) for deprotonation of C4 on the α face or β face by PPi:O1 or PPi:O4 for the different conformations of the ^{TXS}**E** complex. Standard deviations are given in parentheses.[1]

Reaction	Reacting atoms[2]	Reaction energy	Reaction barrier
E_{C_chair} →T	O1-H4β[3]	4.1 (6.8)	53.6 (11.6)
	O4-H4α[4]	0.9 (8.4)	18.0 (7.7)
	O4-H4β[5]	NF[8]	NF[8]
E_{C_boat} →T	O4-H4α[6]	-10.5 (5.0)	7.4 (3.4)
	O4-H4β[5]	-3.9 (8.1)	20.8 (6.9)
$E2_{C\_boat}$ →T	O1-H4β[3]	-13.4 (3.7)	2.7 (1.7)
E_{C_chair} →T1	O1- C20:H[7,5]	-7.4 (3.2)	8.6 (5.9)
E_{C_boat} →T1	O1- C20:H[7,5]	-7.6 (4.1)	8.8 (6.0)

[1] Results are only reported for the setups for which the indicated reaction was found. These setups are specified in the footnotes below. [2] Atom labels can be found in Figures 1 and 3 of the main text.
[3] Average over W1E1, W1E2, and W2E1. [4] Average over W1E2, W2E1 and W2E2C.
[5] Average over W1E1,W2E1, W1E2, W2E2, and W2E2C. [6] Average over W2E2 and W2E2C.
[7] Hydrogen atom closest to base (PPi:O1).
[8] NF = not found; scan does not pass a transition state, but continues to rise in energy (like Fig. S5 right).

Table S12
Average barriers and reaction energies (in kcal/mol) of the expected preferred deprotonation pathway of ^{TXS}**C** (a water-assisted proton transfer to PPi yielding **V**) and of ^{TXS}**F** (deprotonation either directly by PPi or by a water-assisted proton transfer to PPi to produce either **V1** or **V2**). Standard deviations are given in parentheses.[1]

Reaction	Reacting atoms[2]	Reaction energy	Reaction barrier
C →V	C12:H[3]-O_w-O1[4]	-23.4 (2.4)	5.6 (3.0)
F_{chair} →V1	C20:H[3]-O1[5]	-10.7 (2.8)	4.7 (1.3)
F_{boat} →V1	C20:H[3]-O1[6]	-14.4 (0.8)	3.9 (1.5)
F_{boat} →V2	C2:H[3]-O1[7]	-18.2	0.0
F_{boat} →V2	C2:H[3]-O_w-O1[8]	-18.0	1.2
F_{chair} →V2	C2:H[3]-O_w-O1[9]	-18.4 (2.5)	2.5 (1.5)

[1] Results are only reported for the setups for which the indicated reaction was found. These setups are specified in the footnotes below. [2]Atom labels can be found in Figures 1 and 3 of the main text.
[3] Hydrogen atom closest to base (PPi:O1). [4] Average over W1E1,W2E1, W1E2, W2E2, and W2E2C.
[5] Average over W2E1, W2E1F1 and W2E1F2 (two new snapshots of cation **F** taken from MD of ^{TXS}**F**). New snapshots were selected based on cation **F** configuration and the orientation of C20:H and C2:H with respect to O1 to sample all the deprotonation pathways observed during the MD simulation[1]. They are numbered from F1 to F6 and labeled using standard naming conventions for the water network and NTRC orientation, e.g. W2E1F1 has two water molecules between Y835 and PPi:O1 and NTRC orientation E1.
[6] Average over W1E1 and W1E1F3. [7] Data for setup W2E1F4. [8] Data for setup W1E2F5.
[9] Average over W1E1, W1E2, W2E1, W2E2 and W2E2F6.

Table S13
Based on the computed distances, the direct and water-mediated deprotonation by PPi:O1 to side products **V**, **V1** and **V2** seem unlikely for structures on the pathway from the ^{TXS}**E2**$_{C\_boat}$ setup W1E2E.

Proton acceptor-Deprotonation target	**Distance (**Å)	**Water bridge**
PPi:O1-C:C12	7.1	No water molecules within a 4 Å radius
PPi:O1-F_{boat}:C2	5.5	No water molecules within a 4 Å radius
PPi:O1-F_{boat}:C20	4.3	Water bridge between C20:H and PPi but to less basic oxygen (O13)

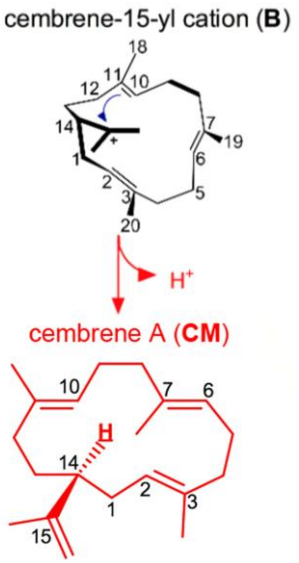

Figure S11 Cembrene A (CM) is a side product observed in the product distribution for mutated TXS. However, in the wild-type product distribution, CM is not detected.[7]

5. Differences between the SHM and the FHM

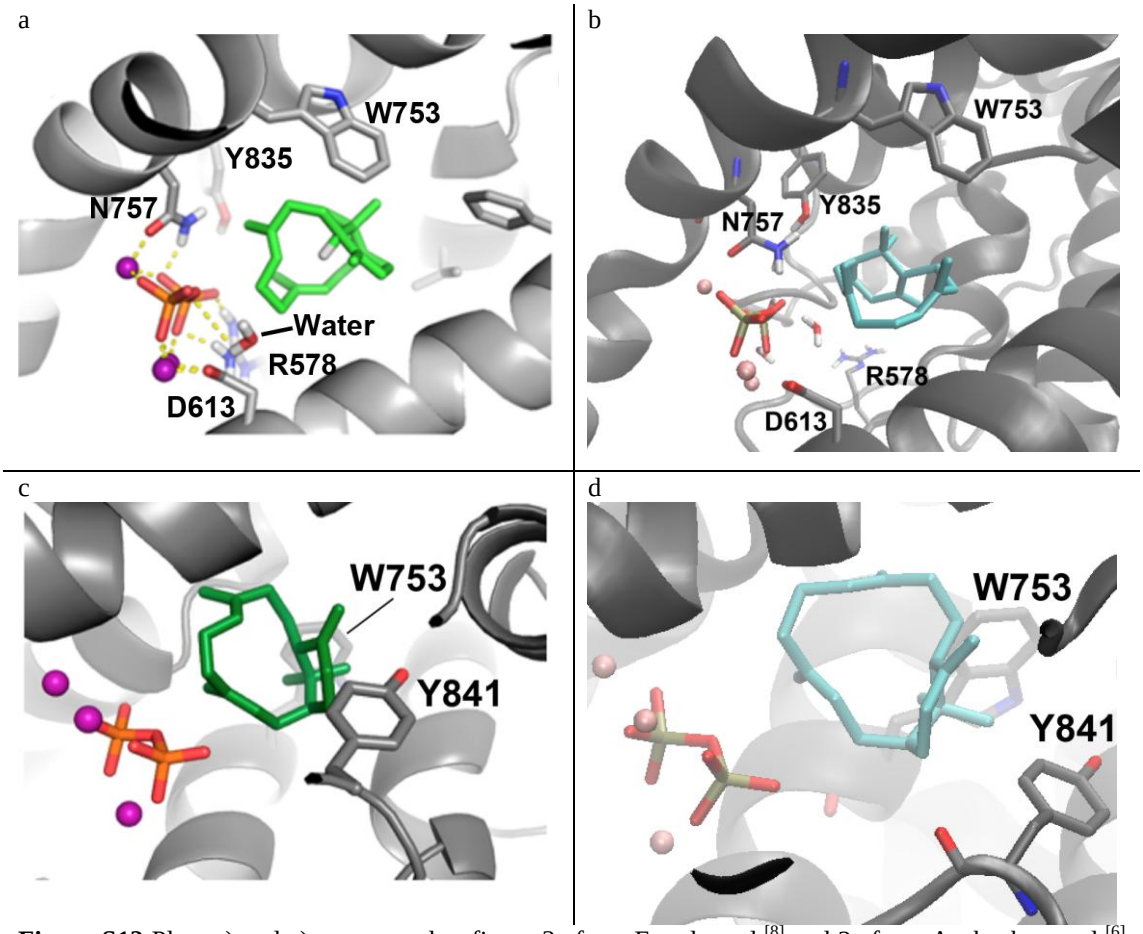

Figure S12 Plots a) and c) correspond to figure 3a from Freud et. al.[8] and 2c from Ansbacher et al.[6] respectively; residue labels have been added. Plots b) and d) depict setup W1E1:**C**; structures have been rotated to facilitate comparison with a) and c). Plots b) and d) highlight the same residues as plots a) and c). In d) water molecules are omitted for clarity.

Number of water molecules

While the setup with the FHM (Fig. S12a) contains a single active-site water molecule, the setup with the SHM (Fig. S12b) has 4 water molecules within 3 Å of the carbocation.

Orientation of the substrate in the binding pocket

The orientation of cation **C** in the binding pocket is very different in Figs. S12a and S12b, while the location and orientation of cation **C** in the binding pocket is similar in Figs. S12c and S12d. Since Figs. S12b and S12d show the same setup, the orientation of cation **C** in Figs. S12a and S12c must be different in the two published studies.[6,8] The differences between our setup and the setup in [6] are significantly smaller than those with setup [8], but they are not negligible. For example, in the FHM from [6] the positive center at ^{TXS}**C**:C11 forms a π−cation interaction with Y841[6] (no distance reported), while in the SHM the $C11^{+}\cdots$Y841 distance is 5.8 Å (see Table S10), so the π−cation interaction is very weak.

Structure of binding pocket

Both R578 (A-C loop) and D839 (J-K loop) are located over 12.5 Å away from PPi in the SHM, while the former residue interacts directly with the PPi moiety in the FHM and the latter makes a water-mediated hydrogen bond with PPi. Therefore it appears that the A–C (G570–H579) and J–K (F837–E846) loops are positioned differently leading to different active-site architectures.

6. References

[1] A. M. Escorcia, J. P. M. van Rijn, G. J. Cheng, P. Schrepfer, T. B. Brück, W. Thiel, *J. Comput. Chem.* **2018**, *39*, 1215–1225
[2] Y. J. Hong, D. J. Tantillo, *J. Am. Chem. Soc.* **2011**, *133*, 18249–18256.
[3] A. M. Escorcia, K. Sen, M. C. Daza, M. Doerr, W. Thiel, *ACS Catal.* **2017**, *7*, 115–127.
[4] P.A. Bash, M. J. Field, R. C. Davenport, G. A. Petsko, D. Ringe, M. Karplus, *Biochemistry*, **1991**, *30*, 5826−583.
[5] J. Gao, X. Xia, *Science*, **1992**, *258*, 631–635.
[6] T. Ansbacher, Y. Freud, D. T. Major, *Biochemistry*, **2018**, *57*, 3773–3779.
[7] P. Schrepfer, A. Buettner, C. Goerner, M. Hertel, J. van Rijn, F. Wallrapp, W. Eisenreich, V. Sieber, R. Kourist, T. Brück, *Proc. Natl. Acad. Sci.* **2016**, *113*, E958-967.
[8] Y. Freud, T. Ansbacher, D. T. Major, *ACS Catal.* **2017**, *7*, 7653–7657.

Reference for Gaussian09:

Frisch, M. J.; Trucks, G. W.; Schlegel, H. B.; Scuseria, G. E.; Robb, M. A.; Cheeseman, J. R.; Scalmani, G.; Barone, V.; Mennucci, B.; Petersson, G. A.; Nakatsuji, H.; Caricato, M.; Li, X.; Hratchian, H. P.; Izmaylov, A. F.; Bloino, J.; Zheng, G.; Sonnenberg, J. L.; Hada, M.; Ehara, M.; Toyota, K.; Fukuda, R.; Hasegawa, J.; Ishida, M.; Nakajima, T.; Honda, Y.; Kitao, O.; Nakai, H.; Vreven, T.; Montgomery, J. A., Jr.; Peralta, J. E.; Ogliaro, F.; Bearpark, M.; Heyd, J. J.; Brothers, E.; Kudin, K. N.; Staroverov, V. N.; Kobayashi, R.; Normand, J.; Raghavachari, K.; Rendell, A.; Burant, J. C.; Iyengar, S. S.; Tomasi, J.; Cossi, M.; Rega, N.; Millam, J. M.; Klene, M.; Knox, J. E.; Cross, J. B.; Bakken, V.; Adamo, C.; Jaramillo, J.; Gomperts, R.; Stratmann, R. E.; Yazyev, O.; Austin, A. J.; Cammi, R.; Pomelli, C.; Ochterski, J. W.; Martin, R. L.; Morokuma, K.; Zakrzewski, V. G.; Voth, G. A.; Salvador, P.; Dannenberg, J. J.; Dapprich, S.; Daniels, A. D.; Farkas, Ö.; Foresman, J. B.; Ortiz, J. V.; Cioslowski, J.; Fox, D. J. Gaussian 09, Revision D.01; Gaussian Inc., Wallingford, CT, 2013.